Bioorganic & Medicinal Chemistry 16 (2008) 9699–9707

Contents lists available at ScienceDirect

Bioorganic & Medicinal Chemistry

journal homepage: www.elsevier.com/locate/bmc

Synthesis and antiviral activity of novel pyrazole derivatives containing oxime esters group

Guiping Ouyang, Zhuo Chen, Xue-Jian Cai, Bao-An Song *, Pinaki S. Bhadury, Song Yang, Lin-Hong Jin, Wei Xue, De-Yu Hu, Song Zeng

Center for Research and Development of Fine Chemicals, Key Laboratory of Green Pesticide and Bioengineering, Ministry of Education, Guizhou University, Guiyang 550025, PR China

ARTICLE INFO

Article history:
Received 20 August 2008
Revised 27 September 2008
Accepted 30 September 2008
Available online 2 October 2008

Keywords:
Pyrazole
Oxime ester moiety
Synthesis
Antiviral bioactivity
Mechanism of action

ABSTRACT

Fourteen title compounds, 1-substituted-5-substitutedphenylthio-4-pyrazolaldoxime ester derivatives **4a**–**4n**, were synthesized from the starting material 1-substitutedphenyl-3-methyl-5-substitutedphenylthio-4-pyrazolaldoximes 3 by treatment with acyl chloride. The synthesized compounds were characterized by physical constants, and the structures of the title compounds were further confirmed by IR, 1H NMR, 13C NMR and elemental analysis. The bioassay results showed that title compounds possessed weak to good anti-TMV bioactivity with **4l** showing significant enhancement of disease resistance in tobacco leaves with high affinity for TMV CP.

1. Introduction

Pyrazole and their derivatives exhibit a broad spectrum of biological activities such as antimicrobial,[1] herbicidal,[2,3] antitumor,[4,5] anti-inflammatory activities.[6–8] Among them, some are used as insecticides, herbicides and fungicides, such as fripronil (Colliot et al., 1992), topramezon (BASF, 2006), pyraelostrobin (BASF, 2001), and so on. With growing application on their synthesis and bioactivity, chemists and biologists in recent years have directed considerable attention on the research of pyrazole derivatives.[7,8]

TMV infection is very widely distributed, and can cause serious damage and large economic loss. It was found that in certain fields 90–100% of the plants show mosaic by harvesting time. Due to the unsatisfactory curatives (30–60%) cure rate by common antiviral agent Ningnanmycin (or Virus A) and economic loss of tobacco, a wide range of chemicals have been synthesized and tested for antiviral effects during screening for biological activity. However, since there are only a few reported economically viable antiviral chemicals available for practical application in agriculture,[9] there still lies a great deal of scope for further research in this field. In view of this, we turned our attention to evaluate the modification of the biological profile induced by the change of the substituents at the 1or 3 or 4 and 5-position in pyrazole ring.

Pyrazolaldoxime esters at 4 position are scarcely evaluated for their antiviral activities. Due to their known fungicidal activities, we reasoned that if oxime esters are linked at 4 position in the pyrazole ring, the resulting compounds will have better bioactivities. Therefore, in our pursuit to develop new class of agrochemicals, we synthesized the title compounds and studied their antiviral activities. The synthetic route is shown in Scheme 1. Starting from the key intermediate 1-substitutedphenyl-3-methyl-5-substitutedphenylthio-4-pyrazolaldoximes **3**, the title compounds **4** are synthesized in one step. Esterification reaction of **3** with acyl chloride affords appropriate oxime ester. The structures of **4** were firmly established by well-defined IR, ^{1}H NMR, ^{13}C NMR and elemental analysis. Preliminary bioassay tests showed that some compounds possess certain degree of antiviral activity against TMV at 500 mg/L in vivo as shown in Table 1, however with a degree of variation. The title compounds **4l** and **4m** had high anti-TMV activities, and the inhibitory effect for the two treated methods ranged from 60.0% to 85.6%. The preliminary studies on action mechanism of compound **4l** against TMV revealed that it was capable to enhance the defense enzyme activity within a certain period and up-regulate PR-1a gene expression. Further studies on the relationship among compound **4l** and TMV CP and TMV RNA showed special affinity of **4l** to CP, but not to RNA. Therefore, we inferred that the action target of compound **4l** against anti-TMV

Abbreviations: ^{1}H NMR, ^{1}H nuclear magnetic resonance; ^{13}C NMR, ^{13}C nuclear magnetic; TMV, tobacco mosaic virus; PAL, L-phenylalanine ammonia-lyase; SOD, superoxide dismutase; POD, peroxidase; SA, salicylic acid; SAR, systemic acquired resistance; PR, pathogenesis-related proteins; PCR, polymerase chain reaction; BLAST, basic local alignment search tool; CP, coat protein.

* Corresponding author. Tel.: +86 851 362 0521; fax: +86 851 362 2211.
E-mail address: songbaoan22@yahoo.com (B.-A. Song).

0968-0896/$ - see front matter © 2008 Elsevier Ltd. All rights reserved.
doi:10.1016/j.bmc.2008.09.070

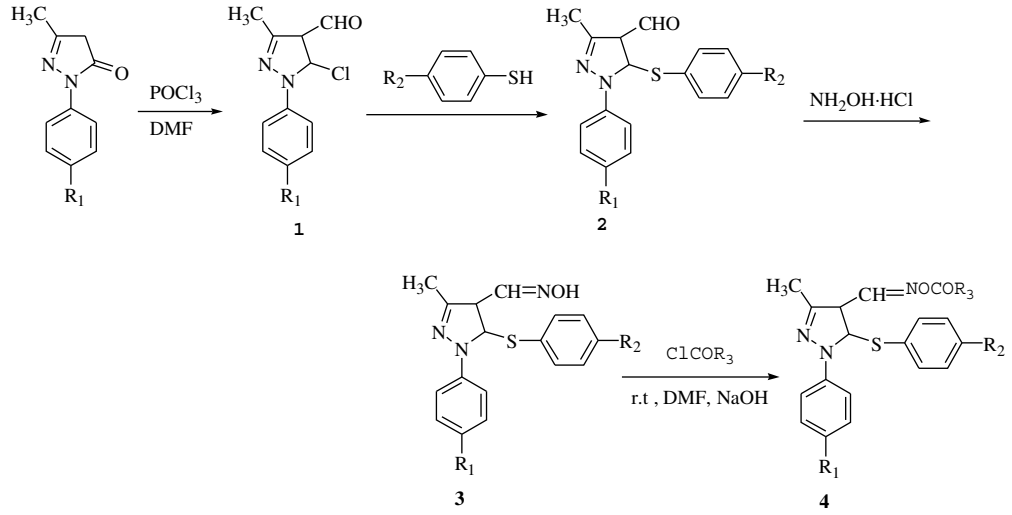

Compd.	R_1	R_2	R_3	Compd.	R_1	R_2	R_3
4a	H	Me	Me	**4b**	H	F	Me
4c	H	F	Ph	**4d**	3-Cl	F	Ph
4e	4-Cl	MeO	Ph	**4f**	4-Me	F	Ph
4g	4-Cl	F	Ph	**4h**	4-Me	F	Me-CH=CH-CH=CH
4i	H	F	Me-$(CH_2)_4$	**4j**	Me	F	Me-$(CH_2)_4$
4k	4-Cl	Me	Me-CH=CH-CH=CH	**4l**	4-Cl	F	Me-$(CH_2)_4$
4m	4-Cl	F	Me-CH=CH-CH=CH	**4n**	H	F	n-Pr

Scheme 1.

was related to up-regulation of the PR gene and promotion of defense enzymes activity to acquire SAR, as well as to limit transfer and proliferation of TMV with highly affinity to CP.

2. Chemistry

2.1. Synthesis of novel pyrazole derivatives

The synthetic route designed for the oxime ester analogues **4** is summarized in Scheme 1. Starting from 1-substitutedphenyl-3-methyl-4-pyrazolone derivatives, the intermediate **1**, 1-substituted phenyl-3-methyl-4-formyl-5-chloropyrazole was prepared by chlorination reaction with $POCl_3$ in DMF. Then, treatment of **1** with substituted thiophenol afforded 1-substitutedphenyl-3-methyl-5-substitutedphenylthio-4-pyrazolaldehyde **2**. Reaction of **2** with hydroxylamine hydrochloride gave 1-substitutedphenyl-3-methyl-5-substitutedphenylthio-4-pyrazolaldoximes **3**. The title compounds, 1-substituted-5-substitutedphenylthio-4-pyrazolaldoxime ester derivatives **4** were synthesized by the esterification reaction of **3** with acyl chloride ($ClCOR_3$).

2.2. Crystal structure analysis

It could be seen from the X-ray single-crystal analysis that title compound **4n** maintains a planar structure. The structure of target compound **4n** was established by X-ray diffraction. The bond lengths of C(7)–C(8) (1.389 Å) and C(8)–C(9) (1.410 Å) are longer than normal C=C (1.34 Å), C(12)–O(1) (1.365 Å) is shorter than normal single C–O (1.44 Å), C(8)–C(11) (1.458 Å) and C(12)–C(13) (1.453 Å) are shorter than normal C–C (1.54 Å), C(11)–N(3) (1.269 Å) and C(3)–N(1) (1.444 Å) bonds are shorter than the normal C–N single bond (1.49 Å), suggesting the existence of an electron density delocalization among O(1)–N(3)–C(11)–C(8)–C(7)–N(1), C(9) and S(1).

3. Antiviral activity

3.1. Preliminary antiviral activity assay

The commercially available plant virucide Ningnanmycin, perhaps the most successful registered anti-plant viral agent available in China, was used as the control. The antiviral bioassay against TMV is assayed by the reported method and the antiviral results of all the compounds against TMV are listed in Table 1. The results showed that most of our designed compounds had moderate to good antiviral activities at 500 mg/L against TMV in vivo.

The title compounds **4a–4n** exhibited good curative activities of 30.0–62.0% at 500 mg/L. Compound **4l** (R_1 was 4-Cl, R_2 was F, and R_3 was Me-$(CH_2)_4$), **4m** (R_1 was 4-Cl, R_2 was F and R_3 was Me–CH=CH–CH=CH) had higher activities (62.0% and 60.0%, respectively) than that of the standard reference (56.0%). In addition, compounds **4a**, **4b**, **4f**, **4g**, **4h** and **4i** showed 40.8–50.0% curative activities at 500 mg/L, with values of 47.8%, 40.4%, 50.0%, 47.7%, 46.7%, and 40.0%, respectively. From the data presented in Table 1, it can be observed that the title compounds **4a–4n** possess potential inactivation bioactivities, with values of 68.3%, 81.4%, 55.0%, 55.0%, 56.8%, 69.2%, 63.8%, 80.2%, 67.8%, 61.5%, 68.9%, 85.6%, 82.9% and 79.9% at 500 μg/mL, respectively. Among these

Table 1
The protection, inactivation and curative effect of the title compounds **4a**–**4n** against TMV in vivo.

Agents	Concentration (mg/L)	Protection effect(%)	Inactivation effect (%)	Curative effect (%)
4a	500	33.8 ± 1*	68.3 ± 3*	47.8 ± 2*
4b	500	36.7 ± 4*	81.4 ± 4**	40.4 ± 3*
4c	500	28.8 ± 3*	55.0 ± 4*	34.9 ± 6*
4d	500	41.0 ± 8*	55.0 ± 6*	30.2 ± 7*
4e	500	27.6 ± 5*	56.8 ± 5*	35.0 ± 6*
4f	500	48.4 ± 7*	69.2 ± 7*	50.0 ± 9*
4g	500	35.0 ± 5*	63.8 ± 9*	47.7 ± 9*
4h	500	26.0 ± 6*	80.2 ± 4**	46.4 ± 3*
4i	500	28.9 ± 5*	67.8 ± 4*	40.2 ± 6*
4j	500	40.9 ± 5*	61.5 ± 3*	30.0 ± 5*
4k	500	50.0 ± 7*	68.9 ± 6*	38.9 ± 4*
4l	500	31.0 ± 6*	85.6 ± 4**	62.0 ± 8**
4m	500	28.3 ± 5*	82.9 ± 5**	60.0 ± 8*
4n	500	25.9 ± 6*	79.9 ± 4**	34.0 ± 3*
Ningnanmycin	500	68.0 ± 5*	97.0 ± 6**	56.0 ± 4*

All results are expressed as means ± SD; $n = 3$ for all groups.
* $P < 0.05$.
** $P < 0.01$.

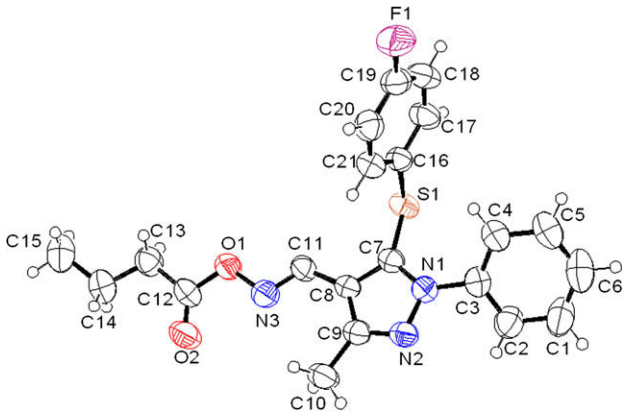

Figure 1. The molecular structure of compound **4n**.

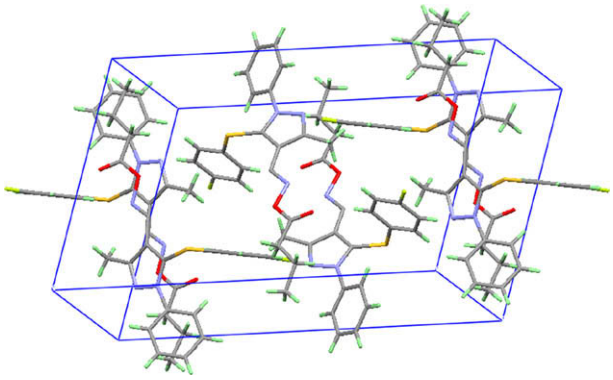

Figure 2. Packing diagram of the unit cell of compound **4n**.

compounds, **4b, 4h, 4l, 4m** and **4n** were appreciably more active than the rest, with the inactivation rates of 81.4%, 80.2%, 85.6%, 82.9% and 79.9%, respectively, which were similar to that of Ningnanmycin (97%) against TMV at 500 μg/mL. The data also indicated that a change in the substituent might also affect the protection activity of title compounds **4a**–**4n**. Compound **4d** (R_1 was 3-Cl, R_2 was F and R_3 was Ph), **4f** (R_1 was 4-Me, R_2 was F and R_3 was Ph), **4j** (R_1 was Me, R_2 was F and R_3 was Me-$(CH_2)_4$]) and **4k** (R_1 was 4-Cl, R_2 was Me and R_3 was Me-CH=CH–CH=CH) had moderate protection activities against TMV of up to 41.0%, 48.4%, 40.9% and 50.0%, respectively, at 500 μg/mL. The other compounds had a relatively lower curative activity than those of **4d, 4f, 4j**, and **4k**.

3.2. Effect of 3l treatment on PAL, POD and SOD activity in tobacco

As shown in Figure 3, using enzyme activity method, PAL, POD, SOD contents in **4l**-treated tobacco showed some definite trend within a certain period of time. POD and SOD levels in **4l**-treated tobacco increased by the end of the first day after the inoculation and reached up to 2.4 EU/mg and 40 EU/mg on the 7th day, respectively, four times greater than the first day after inoculation in enzyme levels. In contrast, in control and TMV, no significant increase was measured. We found that PAL activity in **4l**-treated tobacco decreased from 1st day to 7th day after inoculation, similar trend was not observed on control and TMV.

3.3. Gene expression analysis of PR-1a and PR-5 in 4l-treated tobacco leaf

For the results of product of PCR in PR-1a and PR-5 and their sequence identification, see Supporting information. In vitro synthesized single-stranded cDNA from RNA samples was isolated from leaf in Ningnanmycin-treated tobacco and the TMV-treated tobacco and the **4l** and TMV-treated tobacco. The differential expression analysis of the PR-1a and PR-5 gene was determined by the relative quantification PCR and real-time PCR analysis. As shown in Figure 4, the mRNAs of PR-1a gene accumulated to detectable levels in all-treated tobacco leaf, although, the gene up-regulation in **4l**-treated was found to be higher than the rest from 3rd day to 7th day. The gene expression ratio reached up to 26.6 on the 5th day, the corresponding values for Ningnanmycin-treated and TMV-treated reached only up to 13.85 and 7.64, respectively. The values of compound **4l** were almost twice as large as compared to Ningnanmycin-treated tobacco.

As shown in Figure 5, it could be seen that the mRNA content of **4l**-treated tobacco leaf for PR-5 gene slowly decreased from 1st day to the start of the 3rd day, then gradually increased and reached a peak on the 5th day after the inoculation before showing a gradual decreasing trend again. Meanwhile, similar trends were also observed in TMV-treated, although, for Ningnanmycin-treated tobacco leaf, significant increase in the levels of gene expression ratio was noticed from 3rd day to 5th day, the value reaching up to 17.95. From above results, we found that compound **4l** could induce gene up-regulation of PR-1a without any effect in the regulation of PR-5 gene.

3.4. The primary spectroscopic study of 4l for TMV CP

3.4.1. The ultraviolet–vis spectroscopic study of 4l for TMV CP

For isolation of TMV CP, see Supporting information. The intrinsic UV–vis absorbance peak of CP appeared mainly due to the presence of tryptophan and tyrosine in the CP peptide. As shown in Figure 6, blue line and red line correspond to the UV–vis spectra for TMV CP-treated and TMV CP-**4l**-treated, respectively. It could be seen from the red line in Figure 6A that the absorbance peak values were 2.726 and 0.195 at 207.0 nm and 281.0 nm, respectively, for 4S CP. The absorption peak values of 4S CP shifted toward the longer wavelength side as the compound **4l** was added and the maximum absorption peak increased from 2.726 to 3.136. In addition, the relatively smaller absorption peak

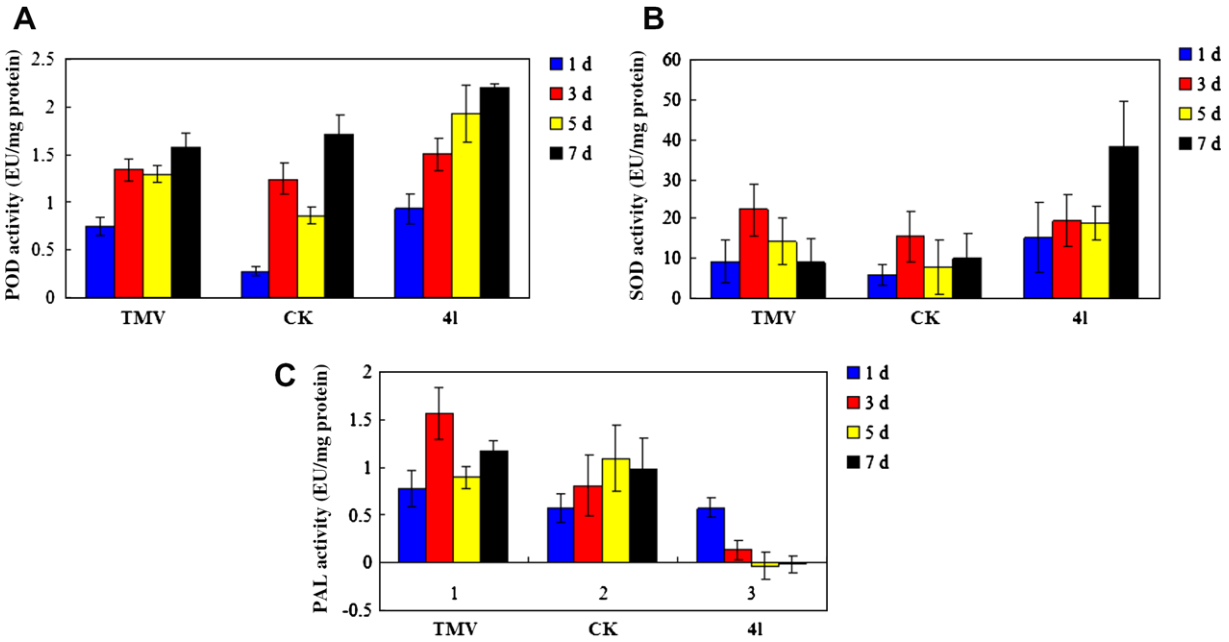

Figure 3. Effect of **4l** treatment on PAL and SOD and POD activity in *Nicotiana tabacum*. *Nicotiana tabacum* inoculated by TMV was treated with **4l** at 500 μg/mL for 1, 3, 5 and 7 day. Leaf sample extracts using homogenized and centrifuged methods were used to determine the PAL and SOD and POD activities as described in Section 6. Water treatment and TMV treatment were used for negative and positive controls. Data were expressed as means ± SD ($n = 3$) of three individual experiments. One-way ANOVA revealed significant difference.

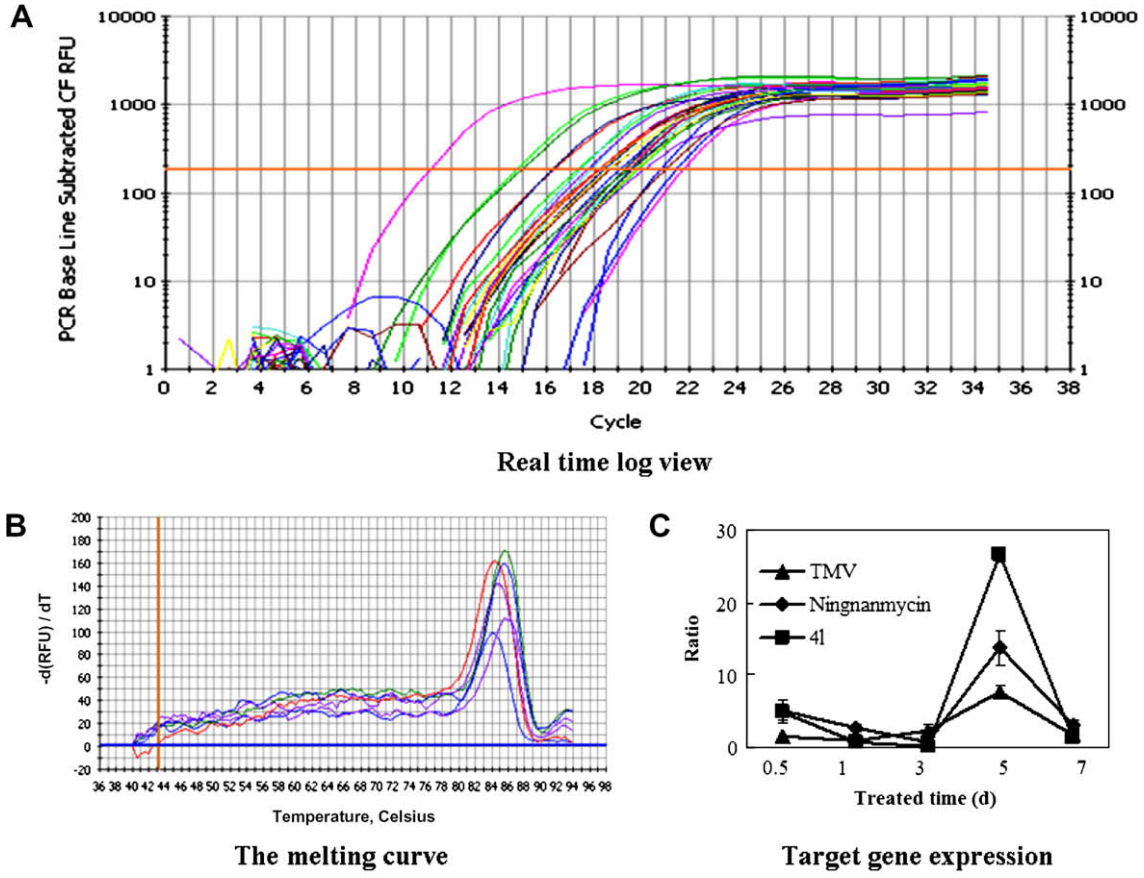

Figure 4. Real-time PCR analysis of RNA isolated from tobacco leaf against PR-1a gene. Letters A in the figures indicate that real-time log view of PR-1a gene. Letters B in the figures indicate that the melting curve of real-time PCR against PR-1a gene. The temperature of the melting curve was 85 °C, the results show the PCR products were purified relatively and had not other non-specific products. Letters C in the figures indicate that the results of PR-1a gene expression ratio through C_T value formula $\Delta\Delta C_T = \Delta C_T$ (test) – ΔC_T (calibrator). Relative values of real-time PCR between target gene and β-actin gene were calculated, each value represents the mean ± SD ($n = 4$) and each experiment was performed in triplicate sets. The data was analyzed by one-way ANOVA.

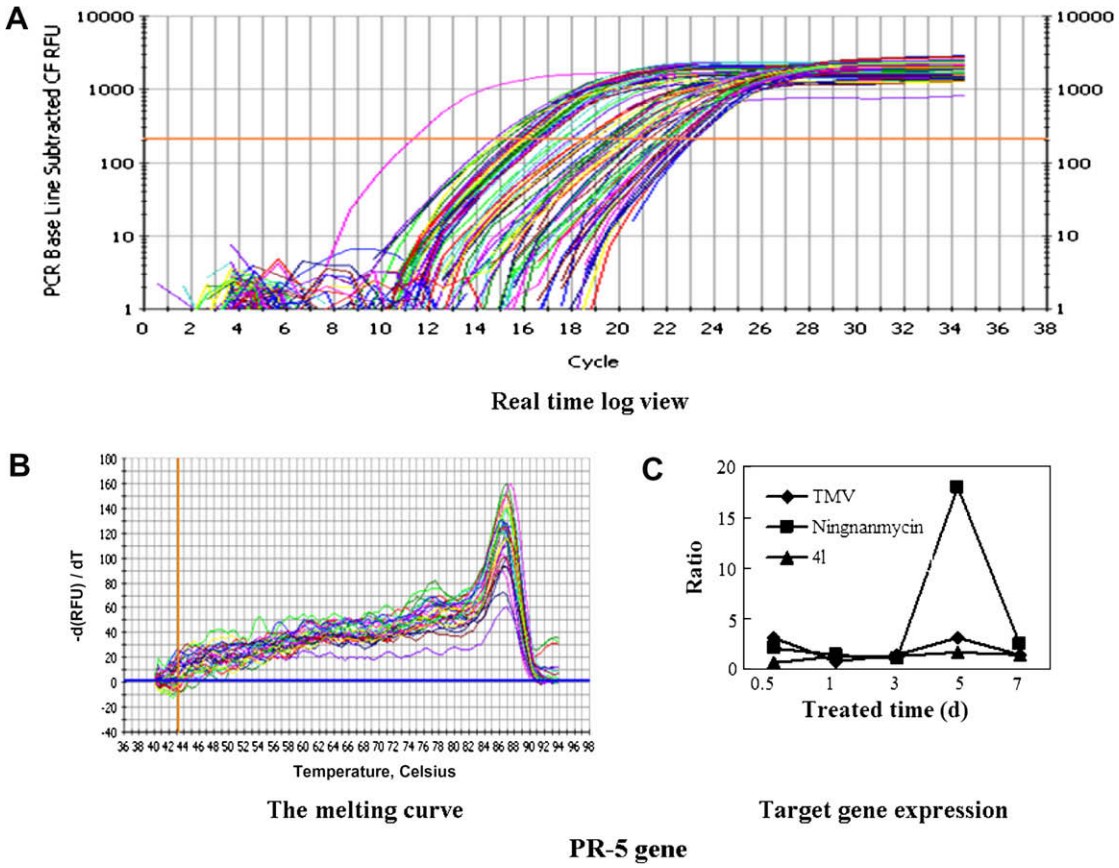

Figure 5. Real-time PCR analysis of RNA isolated from tobacco leaf against PR-5 gene. Letters A in the figures indicate that real-time log view of PR-5 gene. Letters B in the figures indicate that the melting curve of real-time PCR against PR-5 gene. The temperature of the melting curve was 83 °C, the results show the PCR products were purified relatively and had not other non-specific products. Letters C in the figures indicate that the results of PR-5 gene expression ratio through C_T value formula $\Delta\Delta C_T = \Delta C_T$ (test) – ΔC_T (calibrator). Relative values of real-time PCR between target gene and β-actin gene were calculated, each value represents the mean ± SD ($n = 4$) and each experiment was performed in triplicate sets. The data was analyzed by one-way ANOVA.

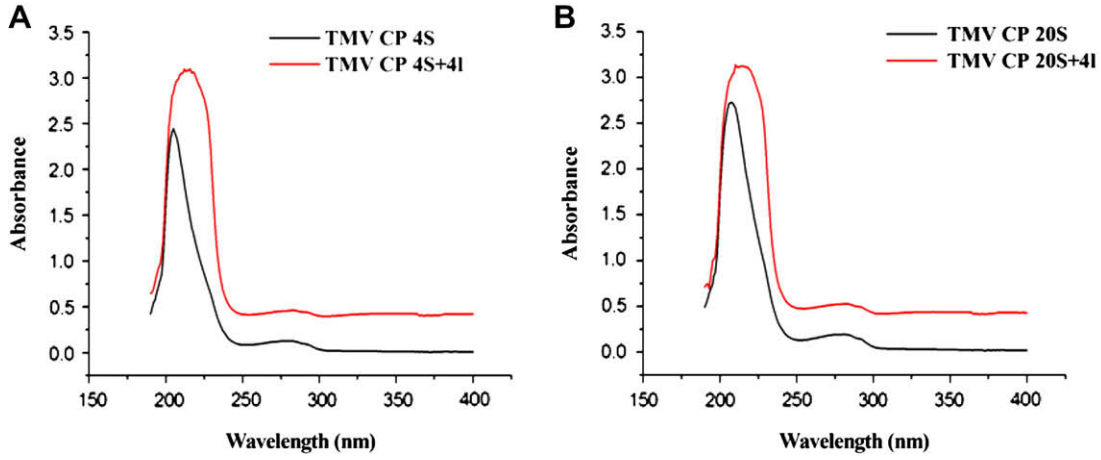

Figure 6. The ultraviolet spectroscopy of TMV CP 4S (A) or 20S (B) protein and **4l**. TMV CP concentration was 0.65 mg/L and concentration of **4l** was varied from 0% to 0.01%.

value shifted slightly toward the longer wavelength side as shown by the blue line in Figure 6A. Similar phenomenon could be observed for TMV CP 20S from Figure 6B. To conclude, as evident from Figure 6, a change in UV–vis spectrum was noticed in the range 190–400 nm as compound **4l** was added, red-shift-phenomenon occurred and peak value increased sharply around 207 and 280 nm. The results indicated that the compound **4l** could associate with CP.

3.4.2. Fluorescence spectroscopic study of 4l for TMV CP

For studying the relationship of compound **4l** with TMV CP, fluorescence spectroscopic assay was used. At 278 nm excitation wavelength, emission wavelength of TMV CP revealed a maximum of emission at 325 nm. As shown in Figure 7A, the excitation wavelengths of TMV CP 4S shifted from 320 to 331 nm as compound **4l** was added, and the fluorescence intensity (a.u.) of TMV CP decreased from 175 to 87. Meanwhile, from Figure 7B, it could be

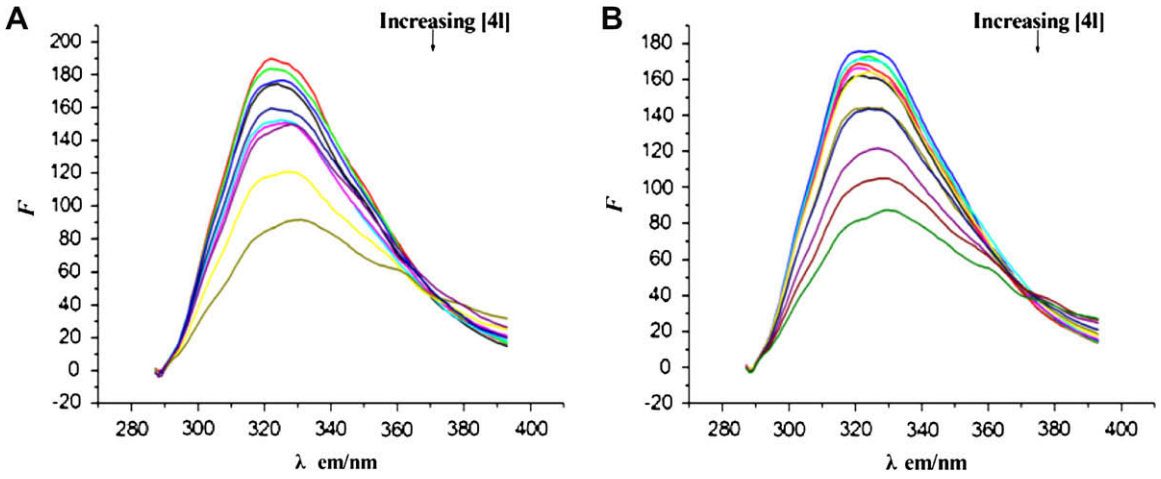

Figure 7. The fluorescence quenching spectra of TMV CP 20S or 4S protein as **4l** is added. 1. 4l = 0 μmol L^{-1}; 2. 4l = 19.952 μmol L^{-1}; 3. 4 l = 39.904 μmol L^{-1}; 4. 4l = 79.808 μmol L^{-1}; 5. 4l = 159.616 μmol L^{-1}; 6. 4l = 203 μmol L^{-1}; 7. 4l = 319.232 μmol L^{-1}; 8. 4l = 464 μmol L^{-1}; 9. 4l = 638 μmol L^{-1}, 10. Curves 1–10: TMV CP = 1.32 μmol L^{-1}. The data was recorded on Fluorescence Spectrophotometer (VARIAN CARY Eclipse) at 250 °C. The excitation wavelength and emission wavelength of TMV CP are 278 nm and 325 nm, respectively. The EX. Slit and EM. Slit and smoothing factor are 5 nm, 5 nm and 10 nm, respectively.

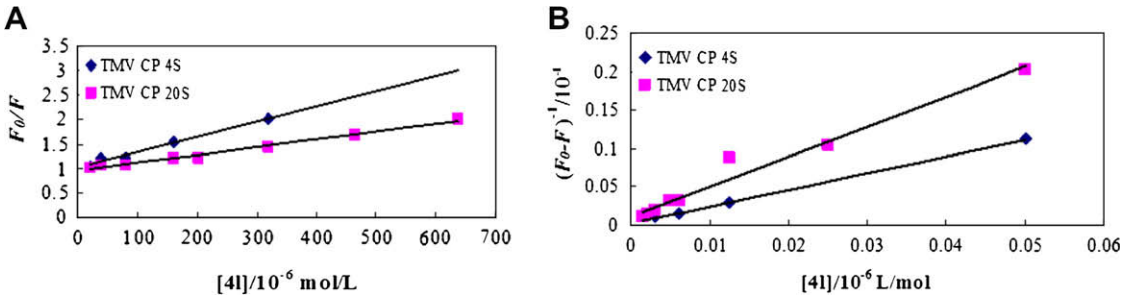

Figure 8. The Stern-Volmer curves (A part) and the double-reciprocal curves (B part) of TMV CP 4S and 20S protein.

Table 2
Regression equations and correlation coefficient.

	Regression equations	R^2
Figure 7A 4S	$F_0/F = 1.0231 + 0.0031 \times 10^4[\mathbf{4l}]$	0.986
Figure 7A 20S	$F_0/F = 0.9608 + 0.0016 \times 10^4[\mathbf{4l}]$	0.9898
Figure 7B 4S	$(F_0 - F)^{-1} = 0.0028 + 2.1681 \times 10^{-7}[\mathbf{4l}]^{-1}$	0.9997
Figure 7B 20S	$(F_0 - F)^{-1} = 0.011 + 3.9027 \times 10^{-7}[\mathbf{4l}]^{-1}$	0.9728

seen that the excitation wavelengths of TMV CP 20S shifted from 321.07 to 330 nm as compound **4l** was added, and the fluorescence intensity (a.u.) of TMV CP 20S decreased from 168.14 to 87.35. From above results, red-shift of wavelengths and fluorescence quenching phenomenon for CP 4S and 20S were noticed when compound **4l** was added. These results also showed that the compound **4l** exhibited a higher affinity for TMV CP.

3.4.3. The determination of quenching constants

The intrinsic fluorescence of TMV CP can be quenched by compound **4l** at 321 and 330 nm. As shown in Figure 8A, F_0/F presented a linear relationship against compound **4l** concentration for TMV CP 4S and 20S protein. From the plot 8A of F_0/F against compound **4l** concentration, the dynamic quenching constants, K_{sv}, were easily calculated from the slope of the straight line, the values were 0.0031×10^4 and 0.0016×10^4 for TMV CP 4S and 20S protein, respectively (Table 2). According to the equation of the constants of collisional quenching rates (K_q), the K_q values were 31×10^8 and 16×10^8 for the above protein. The value was lower than the value of K_q, which is 2.0×10^{10} L mol^{-1} S^{-1} for all the fluorescence quenchers of biomacromolecule. Meanwhile, as shown in plot 8B, the static quenching constants (K_{LB}), were 2.1681×10^{-7} and

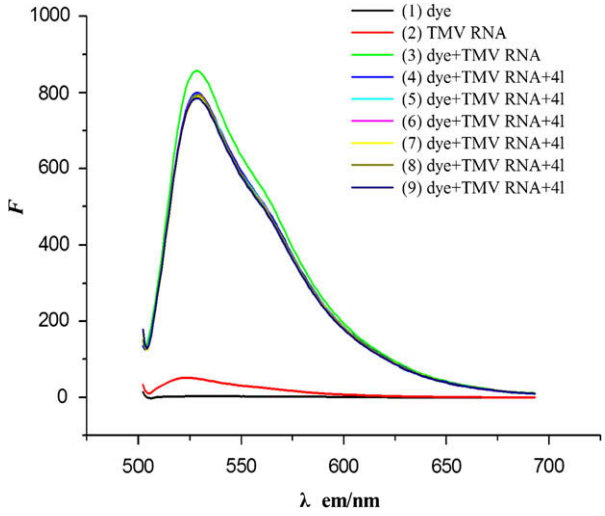

Figure 9. The Fluorescence quenching spectra of TMV RNA as **4l** and cyanine dye are added. 1. Cyanine dye by treated only; 2. TMV RNA by treated only; 3. cyanine dye and TMV RNA by treated; 4–9. the resolution of cyanine dye and TMV RNA as 4l was added. The concentration of **4l** was increased from 19.952 μmol L^{-1} to 159.616 μmol L^{-1}. The data was recorded on Fluorescence Spectrophotometer (VARIAN CARY Eclipse) at 250 °C. The excitation wavelength and emission wavelength of TMV CP are 495 nm and 525 nm, respectively. The EX. Slit and EM. Slit and smoothing factor are 5 nm, 5 nm and 15 nm, respectively.

3.9027×10^{-7} for the above protein (Table 2). Above results suggested a probable binding of compound **4l** with TMV CP mainly through dynamic quenching. The relation between **4l** and TMV CP is worthy of further investigation.

3.5. Fluorescence spectroscopic study of 4l for TMV RNA

For isolation of TMV RNA, see Supporting information. As shown in Figure 9, at 495 nm excitation wavelength, emission wavelength of TMV RNA was 525 nm, the fluorescence intensity of TMV RNA was relatively moderate, and reached up to 52.30 a.u. The fluorescence intensity was lower for cyanine dye, the value being 3.73 a.u. which was close to 0 a.u. When the TMV RNA was mixed with cyanine dye, the fluorescence intensity of the system was increased suddenly, reached to 857.2 a.u. at 528.95 nm for emission wavelength. When compound **4l** was added to the system of TMV RNA and cyanine dye, the fluorescence intensity was not significantly changed but the fluorescence intensity of the system containing compound **4l** was noticed to be comparatively lower. As the differences of the fluorescence intensity were not observed in every concentration group, it was believed that compound **4l** had no effect on TMV RNA.

4. Discussion

With the help of bio-chemistry and molecular biology, significant progress has been made in the antiviral action mechanism studies. At present, we have great understanding about pathogenic mechanism of plant virus and disease resistance mechanism from plant host and pharmacological mechanism of some commercially employed antiviral reagents. Some studies have revealed that the plant defense enzymes[10–12] and some signal transduction pathways mediated by SA and PR can correlate SAR and induce expression by antiviral agents thereby playing an important role in antiviral action mechanism.[13–17] Other studies showed that small natural molecules possessed inhibition activity of plant virus proliferation by specially binding with sub-components of virus against virus nucleic acid or protein.[18] Our results indicate that compound **4l** induced up-regulation of PR-1a gene, the downstream molecule of SA-mediated signal transduction pathway, from 3rd day to 5th day, the corresponding ratio in **4l**-treated tobacco leaf was four times as large as that in TMV-treated tobacco leaf on the 5th day after inoculation. Meanwhile, during 1st day to 7th day, the activity increase of POD and SOD was noticed in compound **4l**-treated, without CK-treated and TMV-treated. So we assumed that compound **4l** possessed the capacity to induce disease resistance. Moreover, using ultraviolet–vis spectroscopic and fluorescence spectroscopic methods, we found that compound **4l** had affinity to TMV CP 4S and 20S protein by induction to red-shift and fluorescence quenching phenomenon, but not to TMV RNA. As TMV CP possessed the ability to protect TMV RNA from digestion by ribonuclease and then help the formation of normal virus particle, antiviral activity of compound **4l** was also thought to be associated with affinity towards TMV CP. So we infer that the antiviral action mechanism might be through a multiply action mode for compound **4l**. Future research would be focused on the study of gene regulation by Northern blot and real-time PCR methods such as pathogenesis-related gene family member, determination of SA content by isolation, extraction and HPLC methods, studies on various molecular levels in SA signaling pathway by gene knock-out and gene knock-in technology, and ascertaining of molecular target sites. Meanwhile, capillary electrophoresistion mode between compound **4l** and TMV CP, the site-directed mutagenesis technology was used to construct the CP peptide containing anticipated amino acids in advance, and analysis of the specific action location of the CP for compound **4l** was made through the single-crystal diffraction and simulation methods to further verification.

5. Conclusion

In conclusion, a series of novel pyrazole derivatives were synthesized by the treatment of 1-substitutedphenyl-3-methyl-5-substituted phenylthio-4-pyrazolaldoximes **3** with acyl chloride. Their structures were verified by spectroscopic data. The results of bioassay showed that these title compounds exhibited weak to good anti-TMV bioactivity. Title compounds **4l**, **4m** showed better biological activity than their structurally related analogues **4a–4k** and **4n**. Preliminary studies showed that treatment by compound **4l** can significantly enhance disease resistance of tobacco and also show that the compound **4l** is structurally related to TMV by exhibiting a higher affinity for TMV CP. So, the action mechanism of curative effect by the compound **4l** was mainly attributed to the induced disease resistance against tobacco while the action mechanism of inactivation effect was caused by its affinity towards TMV CP. More detailed studies on mechanistic aspects are currently underway.

6. Experimental

6.1. Analysis and instruments

The melting points of the products were determined on a XT-4 binocular microscope (Beijing Tech Instrument Co., China) and were not corrected. The IR spectra were recorded on a Bruker VECTOR22 spectrometer in KBr disks. ^{1}H and ^{13}C NMR (solvent DMSO-d_6) spectra were recorded on a JEOL-ECX 500 NMR spectrometer at room temperature using TMS as an internal standard. Elemental analysis was performed on an Elementar Vario-III CHN analyzer. The reagents were all of analytical grade or chemically pure. Analytical TLC was performed on silica gel GF254. Column chromatographic purification was carried out using silica gel. 1-aryl-3-methyl-1H-4-pyrazoleylformaldehydes and 1-(4-chlorophenyl)-3-methyl-1H-4-pyrazolyl-form-aldehydes were prepared according to literature method as described.[19–21] Intermediates 1-aryl-3-methyl-5-chloro-1H-4-pyrazolyl-formaldehydes **1**, **2** and **3** were prepared according to the reported methods.[22]

6.2. Preparation of pyrazolaldoxime ester derivatives (4a–4n)

A 100 mL round-bottomed flask equipped with a magnetic stirrer was charged with **3** (1.5 mmol) and dichloromethane (50 mL) and pyridine (0.012 mol). The flask was stirred at room temperature for 10 min, and then was added drop wise acyl chloride R_3COCl (0.012 mol) dissolved in 20 mL dichloromethane over a period of 0.5 h and refluxed for 4 h. The mixture was cooled and washed with 5% Na_2CO_3 solution and distilled water, dried over anhydrous $MgSO_4$. The solvent was removed and the crude product was purified by chromatography (petroleum ether/ethyl acetate, 2:1) and recrystallized from ethanol to give compound **4** (see the Supporting Information).

6.2.1. 1-Phenyl-3-methyl-5-(4-methylphenylthio)-4-pyrazolaldoxime acetate (4a)

White crystal, mp 90–91 °C, yield, 81%; IR (KBr, cm^{-1}) ν: 3019 (Ar-H), 2975, 923 (CH_3 + CH_2), 1775 (C=O), 1616 (C=N), 1499 (Ar skeleton vibration), 1194 (C=N–N), 801 (*p*-disubstituted benzene), 662 (C–S–C); ^{1}H NMR (DMSO-d_6, 500 MHz, ppm) δ: 8.45 (s, 1H, CH–H), 7.44–7.49 (m, 5H, Ph-H), 7.06 (d, J = 8.05 Hz, 2H, S–Ph-3,5-H), 6.88 (q, J = 8.00 Hz, 2H, S–Ph-2,6-H), 6.87 (t, J = 8.05 Hz,

J = 9.16 Hz 2H, S–Ph-3,5-H); 3.38 (s, 3H, O=C–CH_3–H), 2.2 (s, 3H, pyrazole-CH_3–H), 2.1 (s, 3H, Ph–CH_3–H); ^{13}C NMR (DMSO-d_6, 125 MHz, ppm) δ: 168.9, 149.8, 149.2, 138.7, 137.3, 135.2, 130.7, 130.5, 129.4, 129.2, 128.1, 126.1, 116.9, 20.9, 19.9, 14.9; Anal. Calcd for $C_{20}H_{19}N_3O_2S$ (365.0): C 65.47%, H 5.20%, N 11.50%; found: C 66.55%, H 5.12%, N 10.54%.

6.3. Crystal structure determination

In order to study the single-crystal structure (Figs. 1 and 2), X-ray intensity data were recorded on a Rigaku Raxis-IV diffraction meter using graphite monochromatic MoKα radiation (λ = 0.71073 Å). In the range $1.88° \leqslant \theta \leqslant 27.44°$, 2498 independent reflections were obtained. Intensities were corrected for Lorentz and polarization effects and empirical absorption, and all data were corrected using SADABS program.[23] The structure was solved by direct methods SHELXS-97 program.[24] All the non-hydrogen atoms were refined on $F2$ anisotropically by full-matrix least squares method. The hydrogen atoms were located from the difference Fourier map, but their positions were not refined. The contributions of these hydrogen atoms were included in structure-factor calculations. The final least-square cycle gave wR = 0.1358, R = 0.0517 for 4595 reflection with $I > 2\sigma(I)$; the weighting scheme, $w = 1/[\sigma^2(F_0^2) + (0.00805P)^2 + 0.0458P]$, where $P = [(F_0^2) + 2F_c^2]/3$. The max and min difference peaks and holes were 0.537 and -0.204 e A^{-3}, respectively. s = 1.101. Atomic scattering factors and anomalous dispersion corrections were taken from International Table for X-ray Crystallography.[25] Crystallographic data (excluding structure factors) for the structure have been deposited with the Cambridge Crystallographic Data Center as supplementary publication No. CCDC-696918.

6.4. Protection and inactivation and cure effect of compound against TMV in vivo

Purification of TMV was assessed by Gooding's method, as described in the Supporting Information.[26] The bioactivity assay for protection and inactivation and cure effect was assessed according to Li's method (see the Supporting Information).[27]

6.5. Determination of PAL and POD and SOD activity

The leaf samples were homogenized in the 2-mercaptoethanol-boric acid buffer (5 mM, pH 8.8) on the ice bath and centrifuged. The supernatant was used for experiment. PAL and POD and SOD activities were determined by He's method,[28] Polle's method,[29] Beauchamp's method,[30] respectively (see the Supporting Information).

6.6. RT-PCR assay

Trizol kit was used according to the standard protocol for total RNA isolation. Prior to RT-PCR, the total RNA samples were treated with DNase I for 10 min and quantified by spectrophotometer and identified by agarose gel electrophoresis.[31] cDNA was synthesized with Oligo $(dT)_{18}$ at the 3′ end of mRNA as a primer. Total RNA (1 μg) was used for temple of first-strand cDNA synthesis using extend reverse transcriptase. Reverse transcription was carried out at 37 °C for 1 h. The single-stranded DNA mixture was used as template in PCR. The primers for PCR amplification are shown in Table 3. The PCR was performed in Tris–HCl buffer (10 mM, pH 8.3), KCl (50 mM), $MgCl_2$ (1.8–2.0 μL), dNTPs (0.02 μM), primers (0.04 μM), DNA polymerase (1 U). PCR amplification steps consisted of a preliminary denaturation step at 94 °C for 1 min, followed by 35 cycles at 94 °C for 40 s, at 58 °C for 40 s and at 72 °C for 50 s on icycle of BioRad. PCR products were separated on 1.5% agarose gel in 0.5× TBE buffer and visualized under UV light after staining with ethidium bromide.[32]

Table 3
Sequences of gene-specific primers used in RT-PCR analysis.

Gene family	Accession No.	5′ primer	3′ primer
β-Actin	U60495	5′-gacatgaaggaggagcttgc-3′	5′-atcatggatggctggaagag-3′
PR-1a	X12737	5′-caatacggcgaaaacctagctga -3′	5′-cctagcacatccaacacgaa-3′
PR-5	X03913	5′-gcttccccttttatgccttc-3′	5′-cctgggttcacgttaatgct-3′

6.7. Semi-quantity PCR for expression of gene

In order to assess relative expression levels of target gene in water-treated tobacco and **4l** and TMV-treated tobacco and tobacco by inoculated TMV only, semi-quantity PCR consisting of 20 cycles (within the logarithmic range of amplification of gene) with putting primer of β-actin serving as an internal reference gene was employed for the study. The amplified products were analyzed on a 1.5% agarose gel by the method of Mohamed.[33]

6.8. The relative quantification real-time PCR for expression of the target gene

The relative quantification real-time PCR was carried out with iCycler IQ according to manufacturer's protocol with primer of β-actin serving as an internal reference gene. Precautions were taken to ascertain reliable quantitative results: log-linear dilution curves were performed with primers for the target gene as well as with primers for the β-actin. Reactions performed without reverse transcriptase or without template did not result in any product. By following PCR, 110 steps for melt curve analysis were completed in 10 s at temperature ranging from 40 to 95 °C. The amplification efficiency was 95–99% for PR-1a and PR-5 gene, respectively (the standard curve figures are not shown). Each target gene peak was assigned an arbitrary quantitative value correlated to the β-actin gene peak, according to the formula $\Delta\Delta C_T = \Delta C_{T\,(test)} - \Delta C_{T\,(calibrator)}$, C_T being the cycle threshold. Rates of stimulation of RNA expression were calculated from the ΔC_T values at various time points.[34]

6.9. The primary spectroscopic study of compound 4l for TMV CP

Owing to the presence of tryptophan and tyrosine, protein can emit fluorescence. Therefore, the fluorescence method has sometimes been employed to study the interaction between protein and small drug molecules, the latter being known as fluorescence quencher[35,36] as it can quench the intrinsic fluorescence from the protein. It could be seen that TMV CP containing 3 tryptophan and 5 tyrosine is constituted from 155 amino acids from NCBI protein AAD20291. TMV CP was isolated by acetic acid methods.[37] TMV CP was dissolved in 10 mM phosphate potassium buffer, pH 7.1, 50 mM NaCl. At the concentration of 0.01% of **4l** and 0.65 mg/mL of TMV CP, the interaction between the **4l** and TMV CP ceased to exist and a full spectrum scan was made for the samples in the range 200–600 nm wavelength with ultraviolet spectroscopy. Using fluorescence spectroscopy method, at the resolution of TMV CP 4S and 20S protein at concentration of 1.32 μmol/L, a full spectrum scan to the samples was made in 280–400 nm of wavelength range at 278 nm excitation wavelength.

6.10. The determination of quenching constants

The course of fluorescence quenching was divided into the dynamic quenching and the static quenching.[35] The dynamic quenching involves the interaction between fluorescence quencher and

the excited molecular state of the substance. The action mechanisms accord to the following formulas:

Stern-Volmer equation

$$F_0/F = 1 + K_q\tau_0[Q] = 1 + K_{sv}[Q]$$

Lineweaver-Burk equation

$$(F_0 - F)^{-1} = F_0^{-1} + K_{LB}F_0^{-1}[Q]^{-1}$$

F_0: the fluorescence intensity of substance as the quencher was not added. F: the fluorescence intensity of substance as the quencher was added. [Q]: the concentration of quencher. K_{sv}: the dynamic quenching constants, or the constants of Stern-Volmer. K_q: the constants of collisional quenching rates. K_{LB}: the static quenching constants.

6.11. The primary spectroscopic study of compound 4l for TMV RNA

As RNA contained cyanine dye can emit more intensity of fluorescence than RNA-treated only, some reports employ the fluorescence method to study the interaction between RNA and small drug molecules because quencher, small drug molecules, can competitively bind with RNA, causing cyanine dye to depart from RNA. TMV RNA was dissolved in 10 mM phosphate potassium buffer, pH 7.1, 50 mM NaCl. At the concentration of **4l** varying from 19.952 μmol L^{-1} to 159.616 μmol L^{-1}, the interaction between **4l** and TMV RNA was found to disappear as detected by fluorescence spectroscopy at the excitation and emission wavelength of TMV RNA of 495 nm and 525 nm, respectively.[37]

6.12. Statistical analysis

All statistical analyses were performed with SPSS 10.0. Data were analyzed by one-way analysis of variance (ANOVA). Mean separations were performed using the least significant difference method (LSD test). Each experiment had three replicates and all experiments were run three times with similar results. Measurements from all the replicates were combined and treatment effects analyzed.

Acknowledgments

We are grateful for the financial support from the National Key Project for Basic Research (2003CB114404), Key Technologies R&D Program (2006BAE01A01-15) and the National Natural Science Foundation of China (20562003).

A. Supplementary data

Supplementary data associated with this article can be found, in the online version, at doi:10.1016/j.bmc.2008.09.070.

References and notes

1. Boyne, M.; Stratton, C.; Johnson, F.; Tonge, P. *ACS Chem. Biol.* **2006**, *1*, 43.
2. Vicentini, C. B.; Guccione, S.; Giurato, L.; Ciaccio, R.; Mares, D.; Forlani, G. *J. Agric. Food. Chem.* **2005**, *53*, 3848.
3. Waldrep, T. W.; Beck, J. R.; Lynch, M. P.; Wright, F. L. *J. Agric. Food. Chem.* **1990**, *38*, 541.
4. Pevarello, P.; Brasca, M. G.; Amici, R.; Orsini, P.; Traquandi, G.; Corti, L.; Piutti, C.; Sansonna, P.; Villa, M.; Pierce, B. S.; Pulici, M.; Giordano, P.; Martina, K.; Fritzen, E. L.; Nugent, R. A.; Casale, E.; Cameron, A.; Ciomei, M.; Roletto, F.; Isacchi, A.; Fogliatto, G.; Pesenti, E.; Pastori, W.; Marsiglio, A.; Leach, K. L.; Clare, P. M.; Fiorentini, F.; Varasi, M.; Vulpetti, A.; Warpehoski, M. A. *J. Med. Chem.* **2004**, *47*, 3367.
5. Baraldi, P. G.; Balboni, G.; Pavani, M. G.; Spalluto, G.; Tabrizi, M. A.; Clercq, E. D.; Balzarini, J.; Bando, T.; Sugiyama, H.; Romagnoli, R. *J. Med. Chem.* **2001**, *44*, 2536.
6. Fancelli, D.; Moll, J.; Varasi, M.; Bravo, R.; Artico, R.; Berta, D.; Bindi, S.; Cameron, A.; Candiani, I.; Cappella, P.; Carpinelli, P.; Croci, W.; Forte, B.; Giorgini, M. L.; Klapwijk, J.; Marsiglio, A.; Pesenti, E.; Rocchetti, M.; Roletto, F.; Severino, D.; Soncini, C.; Storici, P.; Tonani, R.; Zugnoni, P.; Vianello, P. *J. Med. Chem.* **2006**, *49*, 7247.
7. Ranatunge, R. R.; Augustyniak, M.; Bandarage, U. K.; Earl, R. A.; Ellis, J. L.; Garvey, D. S.; Janero, D. R.; Letts, L. G.; Martino, A. M.; Murty, M. G.; Richardson, S. K.; Schroeder, J. D.; Shumway, M. J.; Tam, S. W.; Trocha, A. M.; Young, D. V. *J. Med. Chem.* **2004**, *47*, 2180.
8. Goel, A.; Madan, A. K. *J. Chem. Inf. Comput. Sci.* **1995**, *35*, 510.
9. Hansen, A. *J. Crit. Rev. Plant Sci.* **1989**, *8*, 45.
10. Milosevic, N.; Slusarenko, A. *J. Mol. Plant Pathol.* **1996**, *49*, 143.
11. Wang, Y. C.; Hu, D. W.; Zhang, Z. G.; Ma, Z. G.; Zheng, X. B.; Li, D. B. *Physiol. Mol. Plant Pathol.* **2003**, *63*, 223.
12. Sticher, L.; Mauch-Mani, B.; Me′traux, J. P. *Annu. Rev. Phytopathol.* **1997**, *35*, 235.
13. Malamy, J.; Carr, J.; Klessigm, D.; Raskin, I. *Science* **1990**, *250*, 1002.
14. Hahlbrock, K.; Scheel, D. *Plant Mol. Biol.* **1989**, *40*, 347.
15. Rusmussen, J. B.; Hammersschmidt, R.; Zook, M. N. *Plant Physiol.* **1991**, *97*, 1342.
16. Van Loon, L. C. *Plant Mol. Biol.* **1985**, *4*, 111.
17. Tornero, P.; Gadea, J.; Conejero, V. *Mol. Plant Microbe Interact.* **1997**, *10*, 624.
18. Xi, Z.; Zhang, Y. R.; Yu, H. Z.; Ouyang, D. *Bioorg. Med. Chem. Lett.* **2005**, *15*, 2673.
19. Jin, G. Y.; Cao, C. Y.; Li, L. T.; Ren, J. J.; Zhao, G. F. *Chin. J. Pestic. Sci.* **1999**, *1*, 15 (in Chinese).
20. Li, Z. G. *Preparation of Organic Intermediates*; Chemical Industry Press: Beijing, 2001. p 152, 445 (in Chinese).
21. Xu, K. X. *Handbook of Materials and Intermediates of Fine Organic Chemical Industry*; Chemical Industry Press: Beijing, 1998. p 4, pp 4–39 (in Chinese).
22. (a) Xiao, H. Q.; Ouyang, G. P.; Sun, X. D.; Yao, X. D.; Bao, G. Q.; Qi, C. Z. *Chin. J. Syn. Chem.* **2005**, *13*, 600; (b) Ouyang, G. P. Ph.D. Dissertation, Guizhou University, Guiyang, China, 2008.
23. Wilson, A. J.. In *International Table for X-ray Crystallography*; Kluwer Academic Publishers: Dordrecht, 1992; Vol. C,. pp 219–222, 500–502.
24. Sheldrick, G. M. In SHELXTL V5.1, Software Reference Manual; Bruker AXS, Inc: Wisconsin, 1997.
25. Sheldrick, G. M. In *Program for Empirical Absorption Correction of Area Detector Data*; University of Gottingen: Germany, 1996.
26. Gooding, G. V., Jr.; Hebert, T. T. *Phytopathology* **1967**, *10*, 1285.
27. Li, S. Z.; Wang, D. M.; Jiao, S. M. In *Pesticide Experiment Methods—Fungicide Sector*; Li, S. Z., Ed.; Agriculture Press of China: Beijing, 1991; pp 93–94.
28. He, Z. P. In *A Guide to Experiments of Chemical Control for Crops*; He, Z. P., Ed.; Beijing Agricultural University Press: Beijing, 1933; pp 30–31.
29. Polle, A.; Otter, T.; Seifert, F. *Plant Physiol.* **1994**, *106*, 53.
30. Beauchamp, C.; Fridovich, J. *Anal. Biochem.* **1971**, *444*, 276.
31. Yamakawa, H.; Kamada, H.; Satoh, M.; Ohashi, Y. *Plant Physiol.* **1998**, *118*, 1213.
32. Anand, A.; Zhou, T.; Trick, H. N.; Gill, B. S.; Bockus, W. W. *J. Exp. Bot.* **2003**, *54*, 1101.
33. Mohamed, F.; Lydia, F.; Masumi, I.; Hideo, I. *Physiol. Mol. Plant Pathol.* **2004**, *64*, 319.
34. Yuan, J. S.; Reed, A.; Chen, F.; Stewart, C. N. *BMC Bioinform.* **2006**, *7*, 85.
35. Chen, G. Z. *Fluorescence Analytical Method*; Science Press: Beijing, 1990 (in Chinese).
36. The National Center for Biotechnology Information (NCBI). Protein AAD20291.
37. Fraenkel-Conrat, H.; Williams, R. C. *Proc. Natl. Acad. Sci. U.S.A.* **1955**, *41*, 690.